Journal of materials and Environmental Sciences
ISSN : 2028-2508

JMES, 2017 Volume 8, Issue 2, Page 526-538

http://www.jmaterenvironsci.com /

Essential oil *mentha suaveolens L* : Chemical composition, anticorrosive properties on mild steel in 0.5 M H_2SO_4 and chemometric approach

I. Hamdani[1], M. Chikri[2], F. Fethi[2], A. Salhi[1], A. Bouyanzer[1], A. Zarrouk[1], B. Hammouti[3], J. Costa[4], J. M. Desjobert[4]

[1] LC2AME-URAC18, Faculty of Science, First Mohammed University, PO Box 717, 60000 Oujda, Morocco.
[2] Laboratoire de Physique, de la Matière et de Rayonnements (LPMR), Université Mohamed Premier, Faculté des Sciences. Oujda, Morocco.
[3]Laboratory of Nanotechnology, Materials, and the Environment Faculty of Sciences, Université Mohamed V, Rabat, Morocco
[4] Laboratoire de Chimie des Produits Naturels, Faculté des Sciences et Techniques, Université de Corse, UMR CNRS 6134, Corse, France

Received 12 Oct 2016,
Revised 19 Nov 2016,
Accepted 23 Nov 2016

Keywords

- ✓ *Mentha suaveolens L,*
- ✓ GC-MS,
- ✓ Chemometrics,
- ✓ Mild steel,
- ✓ Corrosion inhibition,
- ✓ Electrochemical techniques.

hamdani imad@hotmail.fr

Abstract

The essential oil of *mentha suaveolens L*, was obtained by hydrodistillation and microwave, This oil was analyzed by GC and GC/MS. The analysis of *mentha suaveolens L* oil showed that the major components dtermined by hydrodistillation and Microwave were Piperitenone oxyde (59.3%,73.5%), trans-Caryophyllene (3.7%,3.5%), Germacrene D (3.5%,5.6%), Terpinen-4-ol (3.4 %,1.1%), Nepetalactone (3.2%,0.7%), and p-Cymen-8-ol (2.6%,0.7%), E-hydrate Sabinene (1.6%,2.3%) respectively. Chemometric analysis, including principal component (PCA) was used to determine the best extraction technique to obtain such an element. The *mentha suaveolens L* essential oil (MSLEO) has been evaluated as a corrosion inhibitor for mild steel in 0.5 M H_2SO_4 solution by means of weight loss, potentiodynamic polarization and electrochemical impedance spectroscopy (EIS). Tafel polarization study revealed that *mentha suaveolens L* essential oil (MSLEO) acts as a mixed type inhibitor with predominantly cathodic effect. Adsorption of the inhibitor on the mild steel surface followed Langmuir adsorption isotherm.

1. Introduction

Acidic technology widely used in acid picking and oil-well acidizing results in serious corrosion, becoming a major concern in the oil and gas industry [1]. The injection of organic inhibitors to the aggressive medium has been proven to be an effective and practical way to reduce the corrosion process on metal [2-14]. In particular, organic compounds with suitable structures bearing functional polar electron-donating heteroatoms such as P, S, N or O can serve as efficient corrosion inhibitors [15-28]. The traditional inhibitors, such as synthetic organic compounds, are very effective in reducing corrosion of steels.

Corrosion inhibitors are widely used in industry to reduce the corrosion rate of metals and alloys that are present in contact with aggressive environments [29]. The protective film occurs on the metal surface with a mechanism of adsorption of inhibitors to avoid metals from corrosion, so the surface of the metal and the inhibitor interact with each other. There are two types of corrosion inhibitors: inorganic and organic. The protective action of inorganic inhibitors is related to the formation of oxide film or hardly soluble salt on the metal surface. On the other hand, the protective action of organic inhibitors comes from the adsorption on the oxide films [30]. The most common inorganic inhibitors used for steel are chromates [31,32]. However, because of the high toxicity of chromate, there is a considerable interest in their replacement. Despite the large number of organic compounds, there is always a need for the development of new corrosion inhibitors. So, considerable efforts have been made to find a suitable natural source to be used as a corrosion inhibitor in various corrosive solutions [33]. Because of increasing ecological awareness and strict environmental regulations, as well as the inevitable drive toward sustainable and environmentally friendly processes, attention now has been focused toward the development of nontoxic alternatives to inorganic and organic inhibitors applied so far [34]. There have been many research reports on natural products as corrosion inhibitors in different aggressive environments [37-39]. Several *Mentha* species are used as medicinal herbs, and they are known to possess antimicrobial, insecticidal, antiphlogistic, antiviral, antioxidant, antibacterial, anticancer and antifungal activities [40-45].

In the present work, *mentha suaveolens L* essential oil (MSLEO) is first evaluated as a corrosion inhibitor for mild steel in sulfuric acid. The adsorption and corrosion inhibition of MSLEO are investigated by the of weight loss, potentiodynamic polarization and electrochemical impedance spectroscopy (EIS). The principal component analysis (PCA) was used to exploit the results.

2. **Experimental**

2.1. *Inhibitor*

2.1.1. Plant material

The leaves of *mentha suaveolens* was harvested in May 2015 of the Trifa of the region, in Berkane Eastern Morocco. A voucher specimen was deposited in the Herbarium of Faculty of Sciences, Oujda, Morocco. The dried plant material is stored in the laboratory at room temperature (298 K) and in the shade before the extraction.

2.1.2. Extraction of essential oil

The essential oil of *mentha suaveolens* was isolated by classical hydrodistillation and microwave-assisted hydrodistillation:

- ✓ Hydrodistillation is an extraction method whose function is to extract the volatile compounds of natural products with water vapour, and is often performed using Clevenger-type apparatus (Fig. 1), with 400 g of dried leaves and 400 mL for 3 h. The essential oil yields were measured and subsequently dried over anhydrous sodium sulfate and stored at 277 K in the dark before gas chromatographic determination of its composition.
- ✓ 400 g of dried leaves were hydrodistilled with 400 mL of water by microwave energy (Fig. 1) at 460 W in the multimode reactor fixed at 2450 MHz and equipped by a Clevenger apparatus. The extraction oil was performed at atmospheric pressure for 80 min. The essential oil were dried over anhydrous sodium sulphate yielding and stored in the dark at 277 K until analysis.

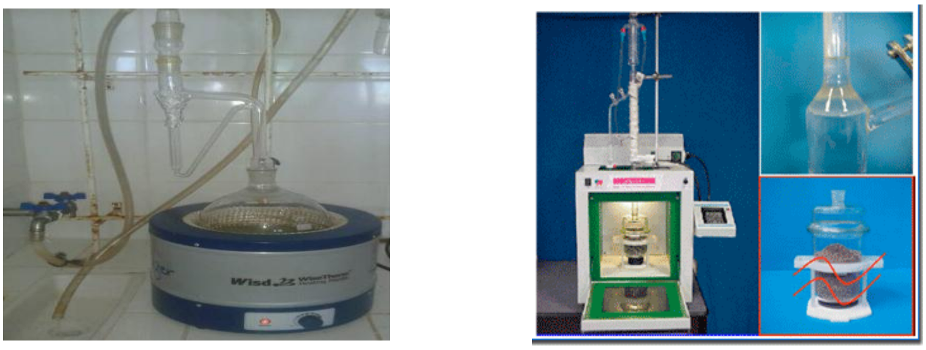

Figure 1: Montage the extraction of essential oil: Classical hydrodistillation (left) and microwave-assisted hydrodistillation (right).

2.1.3. Characterization and chemical composition of essential oil

Techniques in chromatography (GC/MS, GC-FTIR, HPLC-DAD) are available for the molecular analysis of organic compounds. The chemical components of *mentha suaveolens* essential oil was determined by spectral analysis of gas chromatography and gas chromatography coupled to mass spectrometry (GC-MS), which identified six major components. GC analyses were performed using a Perkin-Elmer Autosystem GC apparatus (Waltham, MA, USA) equipped with a single injector and two flame ionization detectors (FID). The apparatus was used for simultaneous sampling with two fused-silica capillary columns (60 m long with i.d. 0.22 mm, film thickness 0.25 µm) with different stationary phases: Rtx-1 (polydimethylsiloxane) and Rtx-Wax (polyethylene glycol). The temperature program was for 333-503K at 275K/min and then held at isothermal 503K (30 min). The carrier gas was helium (1 mL/min). Injector and detector temperatures were held at 553K. Split injection was conducted with a ratio split of 1:80. Electron ionization mass spectra were acquired with a mass range of 35-350 Da. The injected volume of oil was 0.1 µL. For gas chromatography–mass spectrometry, the oils obtained were investigated using a Perkin-Elmer Turbo Mass Quadrupole Detector, directly coupled to a Perkin-Elmer Auto system XL equipped with two fused-silica capillary columns (60 m long with i.d. 0.22 mm, film thickness 0.25 µm), with Rtx-1 (polydimethylsiloxane) and Rtx-Wax (polyethylene glycol). Other GC conditions were the same as described above. Ion source temperature was 423 K and energy ionization 70 eV. Electron ionization mass spectra were acquired with a mass range of 35-350 Da.

The injected volume of oil was 0.1 µL. Identification of the components was based (1) on the comparison of their GC retention indices (RI) on non-polar and polar columns, determined relative to the retention time of a series of n-alkanes with linear interpolation, with those of authentic compounds or literature data [46], and (2) on computer matching with commercial mass spectral libraries [46,47] and comparison of spectra with those in our personal library. Relative amounts of individual components were calculated on the basis of their GC peak areas on the two capillary Rtx-1 and Rtx-Wax columns, without FID response factor correction.

2.2. Materials

The steel used in this study is a mild steel with a chemical composition 0.09 wt. % P; 0.38 wt. % Si; 0.01 wt. % Al; 0.05 wt. % Mn; 0.21 wt. % C; 0.05 wt. % S and the remainder iron (Fe).

2.3. Preparation of solutions

The aggressive solutions of 0.5 M H_2SO_4 were prepared by dilution of analytical grade 98% H_2SO_4 with distilled water. Inhibitor were dissolved in acid solution at the required concentrations, and the solution in the absence of inhibitor is taken as blank for comparison purposes. The test solutions were freshly prepared before each experiment by adding *mentha suaveolens L* essential oil (MSLEO) directly to the corrosive solution. Concentrations of *mentha suaveolens L* essential oil (MSLEO) 0.125, 0.25, 0.5 and 1 g/L.

2.5. Corrosion tests

2.5.1. Gravimetric study

Gravimetric experiments were performed according to the standard methods [48], the mild steel sheets of 1 × 1 × 0.1 cm were abraded with a series of emery papers SiC (120, 600 and 1200) and then washed with distilled water and acetone. After weighing accurately, the specimens were immersed in a 100 mL beaker containing 250 mL of 0.5 M H_2SO_4 solution with and without addition of different concentrations inhibitor. All the aggressive acid solutions were open to air. After 6 h of acid immersion, the specimens were taken out, washed, dried, and weighed accurately. In order to get good reproducibility, all measurements were performed few times and average values were reported to obtain good reproducibility. The inhibition efficiency (η_{WL}%) and surface coverage (θ) were calculated as follows:

$$C_R = \frac{W_b - W_a}{At} \tag{1}$$

$$\eta_{WL}(\%) = \left(1 - \frac{w_i}{w_0}\right) \times 100 \tag{2}$$

$$\theta = \left(1 - \frac{w_i}{w_0}\right) \tag{3}$$

where W_b and W_a are the specimen weight before and after immersion in the tested solution, w_0 and w_i are the values of corrosion weight losses of mild steel in uninhibited and inhibited solutions, respectively, *A* the total area of the mild steel specimen (cm^2) and *t* is the exposure time (h).

2.5.2. Electrochemical measurements

The electrochemical measurements were carried out using Volta lab (Tacussel- Radiometer PGZ 100) potentiostate and controlled by Tacussel corrosion analysis software model (Voltamaster 4) at under static condition. The corrosion cell used had three electrodes. The reference electrode was a saturated calomel electrode (SCE). A platinum electrode was used as auxiliary electrode of surface area of 1 cm^2. The working electrode was mild steel of the surface 0.32 cm^2. All potentials given in this study were referred to this reference electrode. The working electrode was immersed in test solution for 30 min to a establish steady state open circuit potential (E_{ocp}). After measuring the E_{ocp}, the electrochemical measurements were performed. All electrochemical tests have been performed in aerated solutions at 308 K. The EIS experiments were conducted in the frequency range with high limit of 100 kHz and different low limit 0.1 Hz at open circuit potential, with 10 points per decade, at the rest potential, after 30 min of acid immersion, by applying 10 mV ac voltage peak-to-peak. Nyquist plots were made from these experiments. The best semicircle can be fit through the data points in the Nyquist plot using a non-linear least square fit so as to give the intersections with the *x*-axis.

The inhibition efficiency of the inhibitor was calculated from the charge transfer resistance values using the following equation:

$$\eta_{EIS}\,\% = \frac{R_t^i - R_t^{\circ}}{R_t^i} \times 100 \qquad (4)$$

Where, R°_t and R^i_t are the charge transfer resistance in absence and in presence of inhibitor, respectively.
After ac impedance test, the potentiodynamic polarization measurements of mild steel substrate in inhibited and uninhibited solution were scanned from cathodic to the anodic direction, with a scan rate of 1 mV s^{-1}. The potentiodynamic data were analysed using the polarization VoltaMaster 4 software. The linear Tafel segments of anodic and cathodic curves were extrapolated to corrosion potential to obtain corrosion current densities (I_{corr}). From the polarization curves obtained, the corrosion current (I_{corr}) was calculated by curve fitting using the equation:

$$I = I_{corr}\left[exp\left(\frac{2.3\Delta E}{\beta_a}\right) - exp\left(\frac{2.3\Delta E}{\beta_c}\right)\right] \qquad (5)$$

The inhibition efficiency was evaluated from the measured I_{corr} values using the following relationship:

$$\eta_{pp}(\%) = \frac{I_{corr} - I_{corr(i)}}{I_{corr}} \times 100 \qquad (6)$$

where I_{corr} and $I_{corr(i)}$ are the corrosion current densities for steel electrode in the uninhibited and inhibited solutions, respectively.

3. Results and discussion

3.1. Essential oil composition

The essential chemical composition of the oil of *Mentha Suaveolens* by two extraction techniques (hydrodistillation and microwave) was identified and analyzed by GC and GC-MS, he results were summarized in Table 1.

Table 1: GC and GC-MS analysis of essential oil composition from *Mentha Suaveolens L.*

Extraction techniques				**Hydrodistillation**	**Microwave**
Components	**IL**	**Ir /apol**	**Ir /pol**	**%**	**%**
α-Pinene	936	931	1020	0.2	—
Camphene	950	943	1062	0.1	—
1-Octen-3-ol	962	962	1447	1.1	0.2
Sabinene	973	967	1124	0.2	—
β-Pinene	978	971	1107	0.3	—
Myrcene	987	982	1155	0.4	—
α-Terpinene	1013	1011	1182	0.3	—
p-Cymene	1015	1014	1270	0.5	—
Limonene	1025	1023	1199	0.5	—
1,8-Cineole	1024	1023	1211	—	—
Z-β-Ocimene	1029	1027	1233	0.3	—
γ-Terpinene	1051	1050	1211	0.8	—
E-hydrate Sabinene	1053	1055	1461	**1.6**	**2.3**
p-Cymenene	1075	1072	1435	—	—
Terpinolene	1082	1078	1287	0.2	—
Linalol	1086	1085	1544	0.8	0.3
1-Octen-3-yl-acetate		1095	1378	0.7	0.2
cis-p-Menth-2-en-1-ol	1108	1109	1579	0.3	0.1
trans-p-Menth-2-en-1-ol	1123	1125	1559	0.2	—
Borneol	1150	1152	1698	1.6	1.2
Nonanol	1149	1159	1640	—	—

p-Cymen-8-ol	1169	1165	1842	**2.6**	**0.7**
Terpinen-4-ol	1164	1166	1600	**3.4**	**1.1**
Myrtenal	1172	1169	1629	—	—
α-Terpineol	1176	1175	1692	0.6	0.5
Verbenone	1183	1181	1704	—	—
8,9-Dehydrothymol	1190	1197	1986	0.5	0.2
Pulegone	1215	1220	1645	—	—
Piperitone	1226	1229	1732	1.0	—
E-Piperitone oxyde	1232	1233	1703	0.1	—
Z-Piperitone oxyde	1232	1233	1725	0.2	1.0
Bornyl acetate	1270	1272	1579	0.5	0.3
Thymol	1267	1274	2177	—	—
Diosphenol	1276	1280	1801	—	—
Piperitenone	1318	1313	1911	0.7	0.3
Piperitenone oxyde	1335	1339	1949	**59.3**	**73.5**
Z-Jasmone	1371	1371	1935	0.5	0.4
α-Copaene	1379	1380	1495	0.2	0.1
Nepetalactone	1360	1380	1992	**3.2**	**0.5**
β-Bourbonene	1386	1386	1517	0.9	—
β-Elemenene	1389	1390	1592	0.3	0.2
1,2-Epoxymenthyl acetate		1390	1883	—	—
α-Gurjunene	1413	1412	1533	—	—
trans-Caryophyllene	1421	1421	1565	**3.7**	**3.5**
Cadina-3,5-diene	1448	1444	1640	—	—
E–β-Farnesene	1446	1450	1670	0.2	0.3
β-Humulene	1455	1452	1670	0.5	0.4
cis-Muurola-4(15),5-diene	1462	1460	1672	0.3	0.4
Phenethyl 2-methylbutyrate	1468	1467	1967	—	0.2
γ-Muurolene	1474	1473	1690	—	0.2
Germacrene D	1479	1479	1711	**3.5**	**5.6**
Amorpha-4,7(11)-diene	1492	1493	1714	0.1	0.1
α-Muurolene	1496	1495	1719	—	—
γ-Cadinene	1507	1508	1758	0.2	0.2
Calamenene	1517	1512	1829	0.2	0.2
δ-Cadinene	1520	1517	1758	0.3	0.2
α-Cadinene	1534	1532	1733	—	—
Caryophyllene oxyde	1578	1572	1976	0.3	0.2
1-10-diepi-Cubenol	1615	1606	2053	0.2	0.1
τ-Cadinol	1633	1629	2181	0.3	0.1
Hinesol	1632	1632	2190	0.6	0.4
α-Cadinol	1643	1641	2225	0.7	0.2
E-Phytol	2114	2104	2616	—	—
Total				95.2	95.4

IL: Retention indices on the apolar column from literature except those with *.
Ir /apol ; Ir /pol: Retention indices on the apolar Rtx-1 column and on the polar Rtx-Wax, respectively.
All compounds have been identified by GC(RI) and GC-MS from our laboratory library.

Essential oil from aerial parts of *mentha suaveolens* leaves obtained by classical hydrodistillation and microwave-assisted hydrodistillation. The oils were investigated by capillary GC and GC/MS. In total, 63 constituents were identified. 63 compounds were identified in the hydrodistilled oil which accounted for 95.2% of the total oil composition. However, 34 compounds were identified from the microwave-assisted hydrodistillation oil which accounted for 95.2% of the total oil composition.

3.2. Chemometric Method

Principal component analysis [49] involves a mathematical procedure that transforms a number of possibly correlated variables into a smaller number of uncorrelated variables called principal components. The first principal component accounts for as much of the variability in the data as possible, and each succeeding component accounts for as much of the remaining variability as possible. Data sets with many variables can be simplified through variable reduction and thereby be more easily interpreted. In this study the principal component analysis (PCA) was used to exploit the results, build statistical models and determine the appropriate method of extraction of functional groups such as: alcohol, ketone, ester, these characterize the oil quality.

3.2.1. The extraction of monoterpenes and the sesquiterpenes alcohols

Figure 2 shows the result of the ACP which gives the graph of the Scores and the Biplot (Loading-Scores) according to the PC1 vector. We clearly notice that both extraction techniques are well separated (Figure 2a) and the alcohols are highly correlated with the method hydrodistillation and negatively correlated to the microwave method (Figure 2b). This explains the best technique to extract the alcohol is hydrodistillation. This study is paramount to the experimenter to produce the best choice of the experimental plan to extract a good alcohol yield. Just knowing it is needed to trigger the study of corrosion.

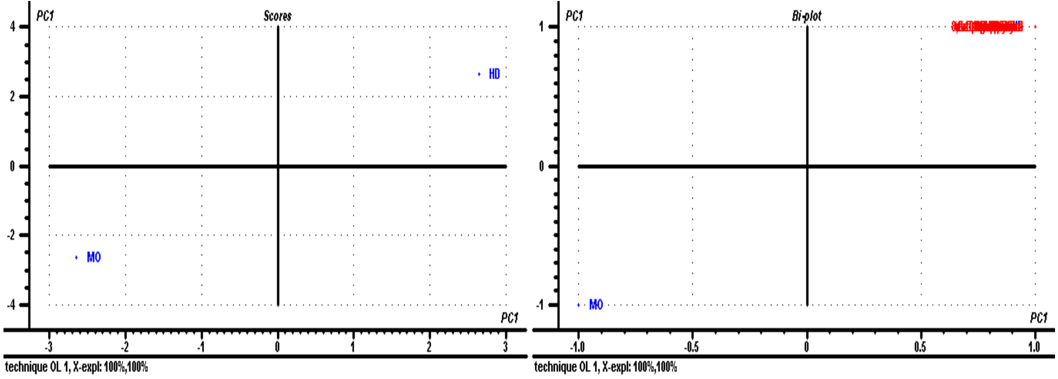

Figure 2: The graph of Scores (PC1 vs.PC1) extraction technique (**a**) and the graph of Biplot (PC1 vs.PC1) showing the analysis of monoterpenes and sesquiterpene alcohols and the extraction technique (**b**).

3.2.2. The extraction of the monoterpene aceton and non-terpene

Figure 3 shows the result of the ACP which gives the graph of the Scores and the Biplot (Loading-Scores) according to the PC1 vector. It is found that the major element (piperitenone) strongly correlates with the microwave extraction method (Figure 3a), by against the other acetones can be extracted by the two techniques since their positions in Figure 3b are between the two extraction methods.

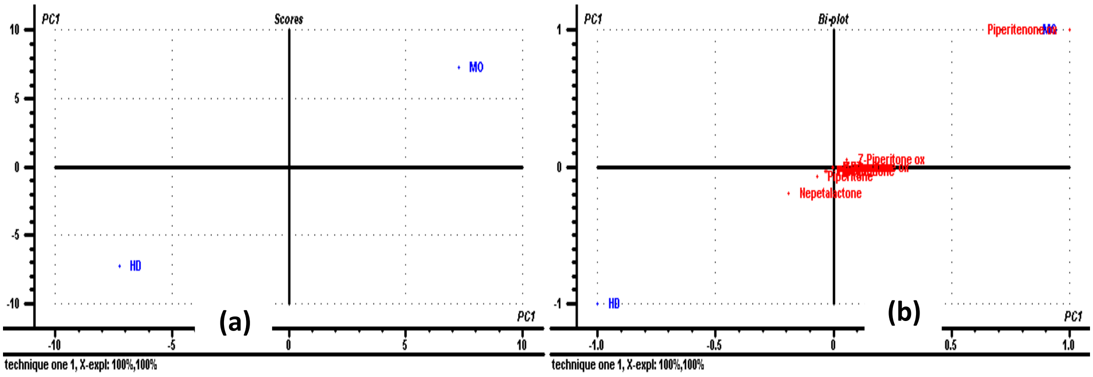

Figure 3: The graph of Scores (PC1 vs.PC1) extraction technique (**a**) and the graph of Biplot (PC1 vs.PC1) showing the analysis of monoterpene acetone and non-terpene and the extraction technique (**b**).

3.2.3. The extraction of the hydrocarbons monoterpenes and the hydrocarbons sesquiterpenes

Figure 4 shows the result of the ACP which gives the graph of the Scores and the Biplot (Loading-Scores) according to the PC1 vector. We clearly notice that the two extraction techniques are well separated and opposite (a) and the two groups are strongly anti-correlated (b). The superposition of the two graphs shows us the best experimental plan to extract the group (I) by the conventional method (hydrodistillation) and the group (II) by the modern method (microwave) (Table 2).

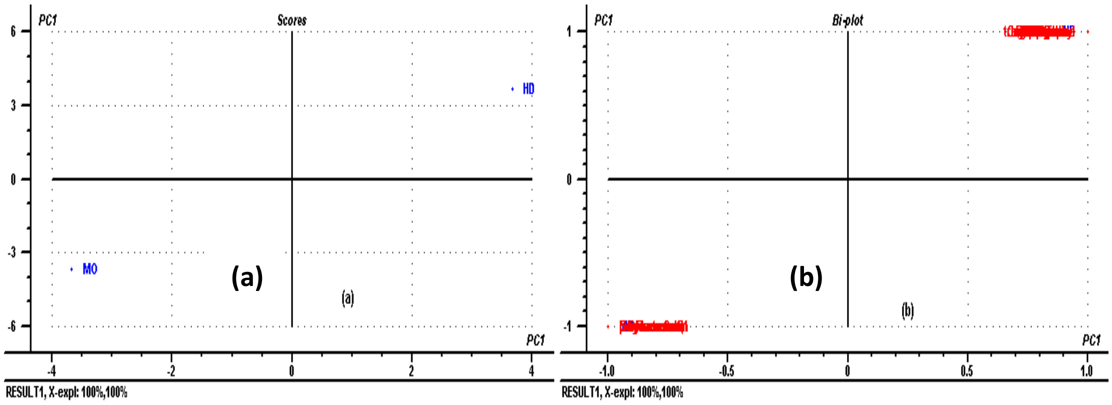

Figure 4: The graph of Scores (PC1 vs.PC1) extraction technique (**a**) and the graph of Biplot (PC1 vs.PC1) showing the analysis of hydrocarbons monoterpenes and hydrocarbons sesquiterpenes and the extraction technique (**b**).

Table 2: Monoterpenes and hydrocarbons Sesquiterpenes are classified in group I and group II respectively.

Group I (hydrocarbons monoterpenes)	Group II (hydrocarbons sesquiterpenes)
α-Pinene;Camphene; Sabinene β-Pinene; Myrcene; γ-Terpinene; p-Cymene; Limonene; Z-β-Ocimene;Terpinolene; α–Copaene; β-Bourbonene; β-Elemenene; α-Gurjunene; trans-Caryophyllene; Cadina-3,5-diene; α-Humulene; γ-Muurolene; α-Cadinene.	E-hydrate Sabinene; p-Cymenene E–β-Farnesene cis-Muurola-4(15),5-diene;GermacreneD;Amorpha-4,7(11)-diene; δ-Cadinene; Calamenene.

3.2.4. The extraction of the terpene oxides

Figure 5 shows the result of the ACP which gives the graph of the Scores and the Biplot (Loading-Scores) according to the PC1 vector. It is found that the two methods are well separated and completely different for the extraction (a). The graph (b) informs us that the best extraction technique piperitone oxide molecule is the microwave

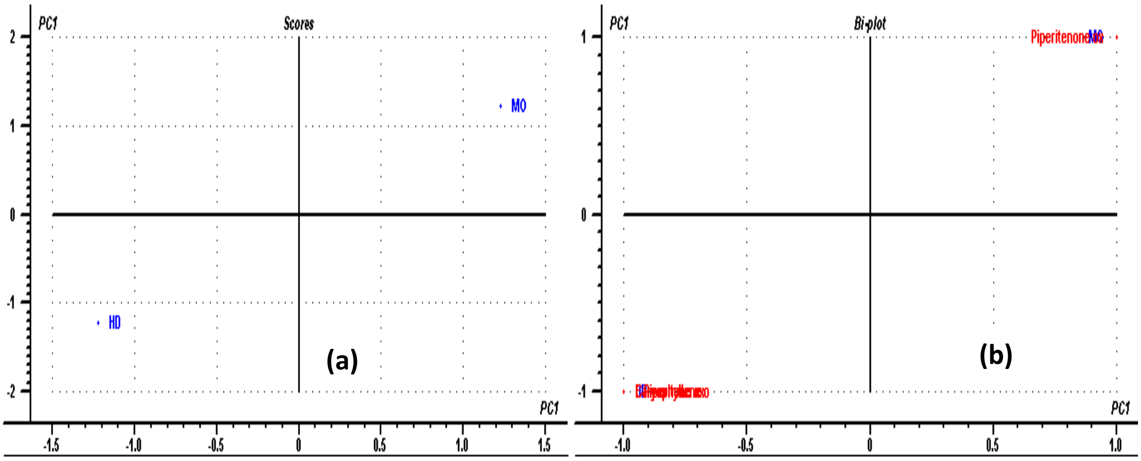

Figure 5: The graph of Scores (PC1 vs.PC1) extraction technique (**a**) and the graph of Biplot (PC1 vs.PC1) illustrating the analysis terpene oxides and the two extraction techniques (**b**).

3.3. Corrosion tests

3.3.1. Electrochemical impedance spectroscopy (EIS)

The Nyquist plots of mild steel obtained in 0.5 M H_2SO_4 solution with various concentrations of *mentha suaveolens L* essential oil (MSLEO) obtained by microwave-assisted hydrodistillation are shown in Figure 6. After analysing the shape of the Nyquist plots, it is concluded that the Nyquist plots showed a depressed capacitive loop in the high-frequency (HF) range and small inductive loop in the low-frequency (LF) range indicating the occurrence of a Faradic process on free electrode sites. The HF capacitive loop can be attributed to the charge transfer reaction and time constant of the electric double layer. On the other hand, the LF inductive loop may be attributed to the relaxation of intermediates controlling the anodic process resulting from adsorption species such as $FeSO_4$ [50], or inhibitor species [51,52] on the electrode surface. It might also be attributed to the redissolution of the passivated surface at LF [53]. Bockris et al. [54] proposed that Fe electro-dissolution in acidic sulphate solutions depends primarily on the adsorbed intermediate $FeOH_{ads}$ as follows:

$$Fe + OH^- \rightleftarrows FeOH_{ads} + H^+ + e \tag{7}$$

$$FeOH_{ads} \xrightarrow{rds} FeOH^+ + e \tag{8}$$

$$FeOH^+ + H^+ \rightleftarrows Fe^{2+} + H_2O \tag{9}$$

The cathodic hydrogen evolution follows the steps:

$$Fe + H^+ \rightleftarrows \left(FeH^+\right)_{ads} \tag{10}$$

$$\left(FeH^+\right)_{ads} + e \rightleftarrows \left(FeH\right)_{ads} \tag{11}$$

$$\left(FeH\right)_{ads} + H^+ + e \rightleftarrows Fe + H_2 \tag{12}$$

The corrosion rate of iron in H_2SO_4 solutions is controlled by both hydrogen evolution reaction and dissolution reaction of iron. Another mechanism involving two adsorbed intermediates has been used to account for the retardation of Fe anodic dissolution in the presence of an inhibitor [55]:

$$Fe + H_2O \rightleftarrows Fe.H_2O_{ads} \tag{13}$$

$$Fe.H_2O_{ads} + Y \rightleftarrows FeOH^-_{ads} + H^+ + Y \tag{14}$$

$$Fe.H_2O_{ads} + Y \rightleftarrows FeY_{ads} + H_2O \tag{15}$$

$$FeOH^-_{ads} \xrightarrow{rds} FeOH_{ads} + e \tag{16}$$

$$FeY_{ads} \rightleftarrows FeY^+_{ads} + e \tag{17}$$

$$FeOH_{ads} + FeY^+_{ads} \rightleftarrows FeY_{ads} + FeOH^+ \tag{18}$$

$$FeOH^+ + H^+ \rightleftarrows Fe^{2+} + H_2O \tag{19}$$

where Y represents the inhibitor species.

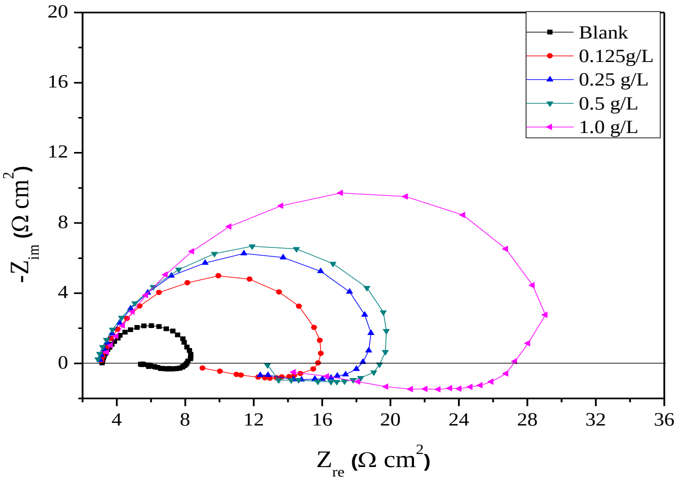

Fig. 6: Nyquist diagrams for mild steel in 0.5M H_2SO_4 containing different concentrations of MSLEO at 308K

The impedance parameters such as charge transfer resistance (R_t: diameter of high frequency loop), derived double layer capacitance (C_{dl}) and inhibition efficiency (η_{EIS} %) are listed in Table 3. The values of the double layer capacitance were obtained at maximum frequency (f_m), at which the imaginary component of the Nyquist plot is maximal, and calculated using the following equation:

$$C_{dl} = \frac{1}{2\pi f_m R_t} \qquad (20)$$

where C_{dl} is the double layer capacitance (µF cm^{-2}), f_m is the maximum frequency (Hz) and R_t is the charge transfer resistance (Ω cm^2). The diameter of the capacitive loop in the presence of inhibitor is larger than that in the absence of inhibitor and increases with the inhibitor concentration. This indicates that the impedance of inhibited substrate increases with the inhibitor concentration.

The existence of the capacitive loops and disappearance of the low-frequency inductive loops when compared with the Nyquist diagram in the 0.5 M H_2SO_4 solutions without inhibitor and in the presence of *mentha suaveolens L* essential oil (MSLEO) could be related to the gradual replacement of water molecules and/or hydroxyl ions by organic inhibitor on the surface of the metal.

It is apparent that as the concentration of the *mentha suaveolens L* essential oil (MSLEO) increased, the R_t values increased indicating decrease in the formation of intermediates that control the anodic process from metal dissolution and subsequently inhibition of corrosion. The increase of charge transfer resistance with the inhibitor concentration suggests that more inhibitor molecules are adsorbed on the metal surface at higher concentration leading to a greater surface coverage. The decrease in the capacity was caused by reduction in local dielectric constant and/or by increase in the thickness of the electrical double layer. This fact suggests that the inhibitor molecules act by adsorption at the metal/ solution interface [56-60].

Table 3: Impedance parameters for mild steel in 0.5 M H_2SO_4 solution in the absence and presence of *mentha suaveolens L* essential oil (MSLEO) at various concentrations.

Conc (g/L)	R_t (Ω cm^2)	f_{max} (Hz)	C_{dl} (µF cm^{-2})	η_{EIS} (%)
Blank	5	200	151	—
0.125	13	158	96	61
0.25	16	158	75	68
0.50	17	158	71	70
1.00	27	158	50	81

3.3.2. Potentiodynamic polarization measurements

Potentiodynamic polarization reflects the impact of corrosion inhibitor on electrode behavior of mi ldsteel in 0.5 M H_2SO_4. The potentiodynamic polarization curves in 0.5 M H_2SO_4 in the presence of different concentrations of *mentha suaveolens L* essential oil (MSLEO) at 308 K were shown in Fig. 7. The electrochemical parameters determined from the polarization curves as corrosion potential (E_{corr}), anodic Tafel slopes (β_a), cathodic Tafel slopes (β_c), corrosion current density (Ic_{orr}) and the inhibition efficiency (η_{PP}) were depicted in Table 4.

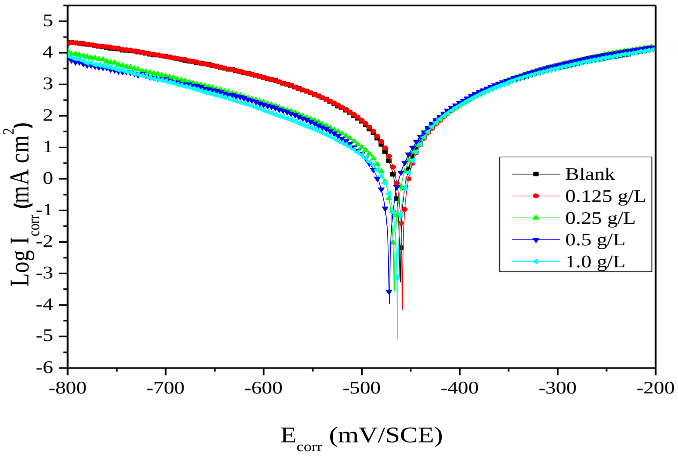

Fig. 7 : EIS diagrams of C38 Steel in 1M HCl at various content of natural oil

It is clearly seen from the Fig. 7 that the nature of polarization curves remains unchanged without and with the inhibitor. The presence of inhibitor only decreases the icorr but does not change the other aspects of the polarization behaviour. The addition of *mentha suaveolens L* essential oil (MSLEO) causes a shift in the values of E_{corr} slightly toward anodic value (more negative) compared to the blank but no definite shift in E_{corr} is detected. The magnitude of change in the E_{corr} values (less than 85 mV) indicate that MSLEO acts as mixed type inhibitor [61] with predominantly cathodic effect, i.e., cathodic evolution of hydrogen gas is more favored than the anodic dissolution of steel. Both β_a and β_c were affected; this was indicative of the mixed-mode inhibitive nature of the inhibitor. The value of I_{corr} decreased progressively with increasing MSLEO concentration. A decrease in I_{corr} suggest that in presence of inhibitor the rate of electrochemical reaction is retarded due to the formation of protective film on the mild steel surface, which created a barrier between metal and corrosive acidic medium.

Table 4: Potentiodynamic polarizations parameters of mild steel in 0.5M H_2SO_4 for various concentrations of MSLEO.

Medium	Conc (g/L)	$-E_{corr}$ (mV_{SCE})	β_a (mV/dec)	$-\beta_c$ (mV/dec)	I_{corr} ($\mu A\ cm^{-2}$)	η_{pp} (%)
Blank	—	461	160.3	177.6	467	—
MSLEO	0.125	459	75.3	80.8	193	58
	0.25	467	58.5	95.5	121	74
	0.50	472	60.0	89.3	106	77
	1.00	464	47.1	96.7	88	81

3.3.3. *Weight loss measurements*

3.3.3.1. *Effect of concentration*

The weight loss method of monitoring corrosion rate and inhibition efficiency is useful because of its simple application and reliability [62]. The values of corrosion rate (C_R) and inhibition efficiency obtained from the weight loss (η_{WL}%) for different *mentha suaveolens L* essential oil (MSLEO) concentrations in 0.5 M H_2SO_4 solutions at 308 K are shown in Table 5. The results show that m decreases noticeably with an increase in *mentha suaveolens L* essential oil (MSLEO) concentration, i.e. the corrosion inhibition enhances with the inhibitor concentration.

This behavior is due to the fact that the adsorption amount and coverage of inhibitor on mild steel surface increase with the inhibitor concentration [63]. It should be noted that when the inhibitor concentration reaches about 1.0 g/L, the corrosion rate value reaches certain data and does not change markedly.

Table 5: Gravimetric results of mild steel corrosion in 0.5 M H_2SO_4 (6 h immersion) without and with various concentrations of MSLEO at 308 K.

Medium	Inhibitor (g/L)	C_R ($mg\ cm^{-2}\ h^{-1}$)	η_{WL} (%)	θ
Blank	—	1.80	—	—
MSLEO	0.125	0.69	61	0.61
	0.25	0.45	75	0.75
	0.50	0.40	78	0.78
	1.00	0.35	80	0.80

3.3.3.2. *Adsorption isotherm*

Generally, inhibition efficiency of inhibitors depends upon degree of adsorption of its constituents on metal surface. But stability of adsorbed molecules (inhibition period) varies with type of adsorption, chemical/physical/both, to a great extent. So, it becomes necessary to study metal-inhibitor interaction through adsorption isotherms. There are many isotherms which are being used to depict adsorption mechanism like Langmuir, Temkin, Frumkin, Flory-Huggins, Freundlich and and thermodynamic/kinetic model of El-Awady isotherm. Efforts were made to fit the results according to these popular isotherms but in our case, we found Langmuir isotherm most suitable to explain adsorption behavior of inhibitor molecules in both acidic medium.

According to Langmuir isotherm [64], surface coverage θ is related to concentration of inhibitor C by following relation:

$$\log\left(\frac{C}{\theta}\right) = \log C - \log K \qquad (21)$$

where C is the equilibrium inhibitor concentration, K_{ads} adsorptive equilibrium constant, θ representing the degree of adsorption (η_{WL}%/100).

The values of regression coefficients ($R^2 = 0.99$) confirmed the validity of this approach. Though the linearity of the Langmuir plot (Fig. 7) may be taken to suggest that the adsorption of inhibitor follows the Langmuir isotherm. For the determination of absorption nature, it is difficult to distinguish between chemisorption and physisorption only based on these criteria, especially when charged species are adsorbed. The possibility of Coulomb interactions between adsorbed cations and specifically adsorbed anions can increase the Gibbs energy even if no chemical bond appears [65]. However, the calculation of the ΔG°_{ads} value of *mentha suaveolens L* essential oil (MSLEO) is not possible because the molecular mass of the extract components is not known. This limitation is noted by some authors in the case of the essential oils used as corrosion inhibitors for steel in acidic media [66,67].

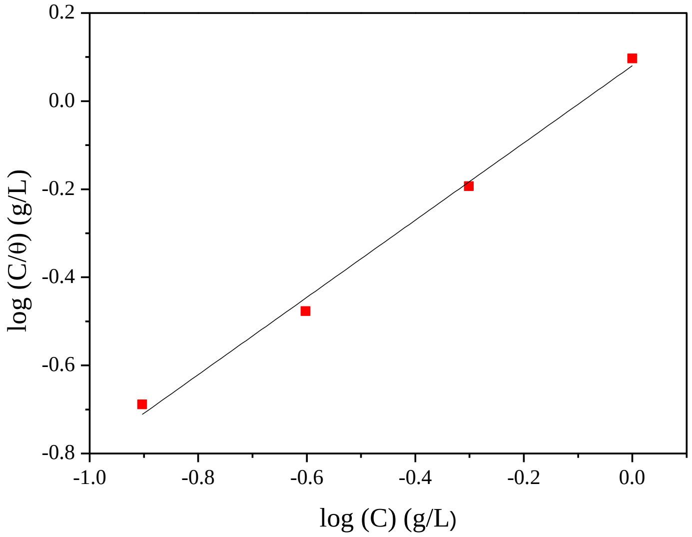

Figure 7: Langmuir adsorption isotherm for mild steel in 0.5 M H_2SO_4 solution of MSLEO at different concentrations by weight loss methods.

Conclusions

In this study, corrosion inhibition efficiency of *mentha suaveolens L* essential oil (MSLEO) on mild steel in 0.5 M H_2SO_4 was determined by weight loss, electrochemical analysis. In the concentration range of 0.125 g/L to 1 g/L, MSLEO shows a good inhibition performance for mild steel in 0.5 M H_2SO_4 solution. The inhibition efficiency of MSLEO increases with increasing inhibition concentration. MSLEO acts as a mixed-typed inhibitor with predominantly cathodic effect, and its adsorption obeys Langmuir adsorption isotherm. Electrochemical impedance spectroscopy data reveals increase in R_t values, which accounted for good inhibition efficiency. Chemometric method allowed elaborating reliable method of quantification for the two principal groups contained in this essential oil.

References

1. Uhlig H. H., Revie R. W., *Corrosion and Corrosion Control*, Wiley, New York, 1985.
2. Nathan C. C., *Organic Inhibitor*, NACE, Houston, TX, 1977.
3. Belayachi M., Serrar H., Zarrok H., El Assyry A., Zarrouk A., Oudda H., Boukhris S., Hammouti B., Ebenso Eno E., Geunbour A., *Int. J. Electrochem. Sci*. 10 (2015) 3010.
4. Zarrok H., Zarrouk A., Salghi R., Ramli Y., Hammouti B., Assouag M., Essassi E. M., Oudda H., Taleb M., *J. Chem. Pharm. Res*. 4 (2012) 5048.
5. Ghazoui A., Bencaht N., Al-Deyab S.S., Zarrouk A., Hammouti B., Ramdani M., Guenbour M., *Int. J. Electrochem. Sci*. 8 (2013) 2272.
6. Ghazoui A., Saddik R., Benchat N., Guenbour M., Hammouti B., Al-Deyab S.S., Zarrouk A., *Int. J. Electrochem. Sci*. 7 (2012) 7080.

7. Ghazoui A., Zarrouk A. , Bencaht N. , Salghi R. , Assouag M. , El Hezzat M. , Guenbour A. , Hammouti B. , *J. Chem. Pharm. Res*. 6 (2014) 704.
8. Zarrok H., Zarrouk A. , Salghi R. , Ebn Touhami M., Oudda H. , Hammouti B., Touir R. , Bentiss F. , Al-Deyab S.S. , *Int. J. Electrochem. Sci*. 8 (2013) 6014.
9. Tayebi H., Bourazmi H., Himmi B., El Assyry A., Ramli Y., Zarrouk A., Geunbour A., Hammouti B., Ebenso Eno E., *Der Pharm. Lett*. 6(6) (2014) 20.
10. Tayebi H., Bourazmi H., Himmi B., El Assyry A., Ramli Y., Zarrouk A., Geunbour A., Hammouti B., *Der Pharm. Chem*. 6(5) (2014) 220.
11. ELaoufir Y., Bourazmi H., Serrar H., Zarrok H., Zarrouk A., Hammouti B., Guenbour A., Boukhriss S., Oudda H., *Der Pharm. Lett*. 6(4) (2014) 526.
12. Zarrouk A., Hammouti B., Dafali A., Zarrok H., *Der Pharm. Chem.* 3 (4) (2011) 266.
13. Zarrouk A., Hammouti B., Zarrok H., Bouachrine M., Khaled K.F., Al-Deyab S.S., *Int. J. Electrochem. Sci.* 6 (2012) 89.
14. Zarrok H., Al Mamari K., Zarrouk A., Salghi R., Hammouti B., Al-Deyab S. S., Essassi E. M., Bentiss F., Oudda H., *Int. J. Electrochem. Sci*. 7 (2012) 10338.
15. Zarrok H., Oudda H., El Midaoui A., Zarrouk A., Hammouti B., Ebn Touhami M., Attayibat A., Radi S., Touzani R., *Res. Chem. Intermed*. 38 (2012) 2051.
16. Zarrok H., Zarrouk A., Salghi R., Oudda H., Hammouti B., Assouag M., Taleb M., Ebn Touhami M., Bouachrine M., Boukhris S., *J. Chem. Pharm. Res*. 4 (2012) 5056.
17. Zarrouk A., Zarrok H., Salghi R., Touir R., Hammouti B., Benchat N., Afrine L.L., Hannache H., El Hezzat M., Bouachrine M. , *J. Chem. Pharm. Res*. 5 (2013) 1482.
18. Zarrok H., Zarrouk A., Salghi R., Assouag M., Hammouti B., Oudda H., Boukhris S., Al Deyab S.S., Warad I., *Der Pharm. Lett*. 5 (2013) 43.
19. Ben Hmamou D., Aouad M.R., Salghi R., Zarrouk A., Assouag M., Benali O., Messali M., Zarrok H., Hammouti B., *J. Chem. Pharm. Res*. 4 (2012) 3498.
20. Belayachi M., Serrar H., El Assyry A., Oudda H., Boukhris S., Ebn Touhami M., Zarrouk A., Hammouti B., Ebenso Eno E., El Midaoui A., *Int. J. Electrochem. Sci*. 10 (2015) 3038.
21. El Hezzat M., Assouag M., Zarrok H., Benzekri Z., El Assyry A., Boukhris S., Souizi A., Galai M., Touir R., Ebn Touhami M., Oudda H., Zarrouk A., *Der Pharm. Chem.* 7(10) (2015) 77
22. EL Arouji S., Alaoui Ismaili K., Zerrouki A., El Kadiri S., Rais Z., Filali Baba M., Taleb M., Emran Khadijah M., Zarrouk A., Aouniti A., Hammouti B., *Der Pharm. Chem.* 7(10) (2015) 67.
23. ELouadi Y., Abrigach F., Bouyanzer A., Touzani R., Riant O., ElMahi B., El Assyry A., Radi S., Zarrouk A., Hammouti B., *Der Pharm. Chem*. 7(8) (2015) 265.
24. Benhiba F., Zarrok H., Elmidaoui A., El Hezzat M., Touir R., Guenbour A., Zarrouk A., Boukhris S., Oudda H., *J. Mater. Environ. Sci*. 6(8) (2015) 2301.
25. Belayachi M., Zarrok H., Larouj M., Zarrouk A., Bourazmi H., Guenbour A., Hammouti B., Boukhriss S., Oudda H., *Phys. Chem. News* 74 (2014) 85.
26. El Azzouzi M., Aouniti A., Tighadouin S., Elmsellem H., Radi S., Hammouti B., El Assyry A., Bentiss F., Zarrouk A., *J. Mol. Liq.* 221 (2016) 633.
27. Tazouti A., Galai M., Touir R., Ebn Touhami M., Zarrouk A., Ramli Y., Saraçoğlu M., Kaya S., Kandemirli F., Kaya C., *J. Mol. Liq.* 221 (2016) 815.
28. Bouanis M., Tourabi M., Nyassi A., Zarrouk A., Jama C., Bentiss F., *Appl. Surf. Sci.* 389 (2016) 952.
29. Gerengi H., Darowicki K., Bereket G., Slepski P., *Corros. Sci.* 51 (2009) 2573.
30. Bereket G., Yurt A., *Corros. Sci.* 43 (2001) 1179.
31. Zhao J.M., Zuo Y., *Corros. Sci.* 44, (2002) 2119.
32. Levbare G. O., Burstein G. T., *Corros. Sci.* 45 (2003) 1545.
33. Rosliza R., Wan Nik W. B., *Curr. Appl. Phys.* 10 (2010) 221.
34. Gerengi H., Sahin H. I., *Ind. Eng. Chem. Res*. 51 (2012) 780.
35. Hamdani I., El Ouariachi E., Mokhtari O., Salhi A., Bouyanzer A., Zarrouk A., Hammouti B., Costa J., *Der Pharm. Lett*. 7(9) (2015) 109.
36. Lotfi N., Benhiba F., Chahboun N., Bourazmi H., El Hezzat M., Al Hamzi A.H., Zarrok H., Guenbour A., Ouhssine M., Oudda H., Zarrouk A., *Der Pharm. Lett*. 7(9) (2015) 1.
37. Hamdani I., El Ouariachi E., Mokhtari O., Salhi A., Chahboun N., ElMahi B., Bouyanzer A., Zarrouk A., Hammouti B., Costa J., *Der Pharm. Chem*. 7(8) (2015) 252.
38. Rekkab S., Zarrok H., Salghi R., Zarrouk A., Bazzi Lh., Hammouti B., Kabouche Z., Touzani R., Zougagh M., *J. Mater. Environ. Sci*. 3 (2012) 613.

39. Ben Hmamou D., Salghi R., Zarrouk A., Al-Deyab S.S., Zarrok H., Hammouti B., Errami E., *Int. J. Electrochem. Sci*. 7 (2012) 6234.
40. Brahmi F., Abdenour A., Bruno M., Silvia P., Alessandra P., Danilo F., Drifa Y-G., Fahmi E.M., Khodir M., Mohamed C., *Ind. Crops Prod.* 8 (2016) 96.
41. Benayad N., Ebrahim W., Hakiki A., Mosaddak M., *Scientific Study and Research: Chemistry and Chemical Engineering, Biotechnology, Food Industry*, 13 (2012) 27.
42. Dorman H.J.D., Kosar M., Kahlos K., Holm Y., Hiltunen R., *J. Agric. Food. Chem.* 51 (2003) 4563.
43. Adam K., Sivropoulou A., Kokkini S., Lanaras T., Arenakis M., *J. Agric. Food. Chem.* 46 (5) (1998) 1739.
44. Oumzil H., Ghoulami S., Rhajaoui M., Ilidrissi A., Fkih-Tetouani S., Faid M., Benjouad A., *Phytother. Res.* 16 (8) (2002) 727.
45. Singh R., Shushni M.A.M., Belkheir A., *Arab. J. Chem*. 8 (3) (2015) 322.
46. Bouyanzer A., Hammouti B., L. Majidi, *Mater. Letters* 60 (2006) 2840.
47. Bouyanzer A., Majidi L., Hammouti B., *Bull. Elect.* 22 (2006) 321.
48. ASTM, G 31-72, American Society for Testing and Materials, Philadelphia, PA, 1990.
49. Wold S., Esbensen K., Geladi P., *Chemometr. Intell. Lab.* 2 (1987) 37.
50. Keddam M., Mattos O.R., Takenouti H., *J. Electrochem. Soc.* 128 (1981) 266.
51. Epelboin I., Gabrielli C., Keddam M., Takenouti H., *Compr. Treatise. Electrochem.* 4 (1981) 151.
52. Al Mamari K., Elmsellem H., Sebbar N. K., Elyoussfi A., Steli H., Ellouz M., Ouzidan Y., Nadeem A., Essassi E. M., El-Hajjaji F., *J. Mater. Environ. Sci.* 7 (9) (2016) 3286-3299
53. Sherif E.M., Park S.M., *Electrochim. Acta* 51 (2006) 1313.
54. Bockris J.O.M., Drazic D., Despic A.R., *Electrochim. Acta* 4 (1961) 325.
55. Ashassi-Sorkhabi H., Nabavi-Amri S.A., *Acta. Chim. Slov.* 47 (2000) 507.
56. Osman M.M., *Anti. Corros-Methods Mater.* 45 (1998) 176.
57. Reinhard G., Rammelt U., Proceedings of the 6th European symposium on corrosion inhibitors, Ferrara, Italy, p 831, (1985).
58. Growcock F.B., Jasinski R.J., *J. Electrochem. Soc.* 136 (1989) 2310.
59. Kissi M., Bouklah M., Hammouti B., Benkaddour M., *Appl. Surf. Sci.* 252 (2006) 4190.
60. Econway B., Bai L., *Electrochim. Acta* 31 (1986) 1013.
61. Ghazoui A., Benchat N., El-Hajjaji F., Taleb M., Rais Z., Saddik R., Elaatiaoui A., Hammouti B., *J. Alloys Comp.*, 693 (2017) 510-517
62. Li X., Deng Sh., Fu H., Corros. Sci. 53 (2011) 302.
63. Li X.H., Mu G.N., *Appl. Surf. Sci.* 252 (2005) 1254.
64. Avci G., *Colloids and Surfaces A: Physicochem. Eng. Aspects*. 317 (2008) 730.
65. Singh A.K., Quraishi M.A., *Corros. Sci*. 53 (2011) 1288.
66. ElHajjaji F., Greche H., Taleb M., Chetouani A.,, Aouniti A., Hammouti B., *J. Mater. Environ. Sci.* 7 (2) (2016) 566-578.
67. Faustin M., Maciuk A., Salvin P., Roos C., M. Lebrini, *Corros. Sci.* 92 (2015) 28.

(2017) ; http://www.jmaterenvironsci.com